Microstructure Fiber Soliton Laser

Mathias Moenster, Peter Glas, Rumen Iliew, Reiner Wedell, and Günter Steinmeyer, *Member, IEEE*

Abstract—We demonstrate femtosecond pulse operation of a soliton fiber laser at 1.06-μm wavelength. This laser makes use of a single piece of microstructure fiber that has been designed to simultaneously provide anomalous dispersion and laser gain. Using a saturable absorber mirror with deep modulation depth to initiate and sustain mode-locking, this fiber provides clean and nearly transform-limited pulses down to a pulse duration of 180 fs. To the best of our knowledge, this constitutes the first demonstration of a pure soliton fiber laser in the neodymium gain band.

Index Terms—Femtosecond pulse generation, fiber lasers, microstructure fiber (MSF), neodymium, passive mode-locking, saturable absorber mirrors (SAMs), solitons.

Fig. 1. Laser setup. DM: dichroic mirror. L: aspheric lens, $f = 8$ mm. M: output coupler. W: 1° wedge, oriented at Brewster's angle for polarization selection. Nd : MSF: neodymium-doped MSF. Ti : Sa: Ti : sapphire pump laser, operating at 808 nm in CW operation. The inset shows an SEM micrograph of the Nd : MSF endface.

MODE-LOCKED fiber lasers have a range of properties that often makes them the preferred choice for a laser oscillator. Femtosecond fiber lasers are extremely compact, they can be ruggedized and shielded from environmental influences for low-noise applications, which makes them a particular interesting type of laser for use in frequency metrology [1]. Nevertheless, femtosecond operation of fiber lasers has been widely restricted to the erbium gain bandwidth at 1.5-μm wavelength [2]. Even though fibers can easily be doped with ytterbium or neodymium ions to provide gain at shorter wavelengths, dispersion management using traditional fibers is virtually impossible below 1.3-μm wavelength. Instead, however, one can integrate bulk optics into the laser cavity for dispersion compensation [3]. Here we demonstrate use of microstructure fibers (MSFs) [4], [5] to provide anomalous dispersion for soliton formation together with laser gain at 1.06-μm wavelength. In contrast with previous studies [6], [7] that combined pieces of microstructured fiber with conventional rare-earth doped fiber sections, we provide gain and dispersion control in a single type of fiber; enabling the existence of bright soliton solutions in the entire fiber length of our cavity. Using this fiber together with a saturable absorber mirror (SAM) in a laser cavity gives rise to the formation of stable and nearly transform-limited femtosecond pulses. Another benefit of our approach is the scalability of the cavity length toward high repetition rates. Besides the saturable absorption provided by the SAM, all other mechanisms required for mode-locking are integrated in the MSF.

Fig. 1 shows the experimental setup together with a scanning electron micrograph (SEM) of the fiber cross section used in our laser. The fiber structure consists of a hexagonal arrangement of air holes with 0.8-μm diameter at a 1.8-μm pitch surrounding a central defect. This core area is doped with 4500-ppm Nd_2O_3 and supports a guided mode with an effective area of 4 μm^2 at 1.06 μm. The fiber is manufactured from a soft phosphate glass, which greatly facilitates drawing of the fiber, allowing for some fine-tuning of the geometric and dispersive properties of the fiber for optimum performance at the Nd wavelength. Phosphate glasses allow for a very high doping concentration of Nd ions which enables very short pump absorption lengths, and therefore, higher repetitions rates. Moreover, phosphate glass is known for an increased Kerr nonlinearity resulting in a nonlinear index of refraction $n_2 \approx 6 \times 10^{-16}$cm^2/W [8], i.e., about twice the value of pure fused silica. This results in a fiber nonlinearity $\gamma = 90$ W^{-1}·km^{-1}. The dispersion characteristics of the fiber have been computed numerically as $\beta_2 = -20$ ps^2/km at a wavelength of 1.06 μm. This result has been independently checked by spectral interferometry measurements, yielding a slightly different value $\beta_2 = -15$ ps^2/km.

A 56-cm-long segment of this fiber is inserted into a linear cavity with a 20% output coupler in one arm and an SAM in the other. The fiber end faces were sealed with the procedure described in [8]. For pumping, a continuous-wave (CW) Ti : sapphire laser is used at 808 nm with a typical launched pump power of 20 mW inside the fiber. We employ a hybrid cavity setup with air paths in between the elements, mainly as it allows independent adjustment of the spot size on the SAM. We use $f = 8$ mm molded aspheric lenses for coupling and focusing on to the SAM. Polarization selection in the cavity is accomplished by either inserting a slightly wedged plate near Brewster's angle or a dichroic glass polarizer. We used three different SAMs in our experiments, which we will refer

TABLE I
MEASURED PROPERTIES OF THE SAMs USED IN THIS STUDY

SAM	ΔR	ΔR_{ns}	F_{sat}	τ_r
1	0.42	0.13	$110\,\mu J/cm^2$	1 ps
2	0.16	0.11	$160\,\mu J/cm^2$	300 fs
3	0.15	0.05	$50\,\mu J/cm^2$	10 ps
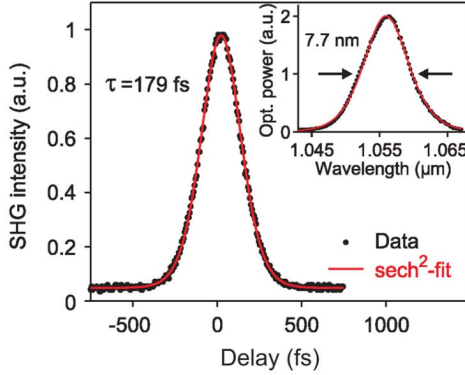
Fig. 2. Autocorrelation and spectrum (inset) measured with SAM 1. Dots: measured data. Solid curves: hyperbolic secant fit to the measured data. The pulse duration τ (FWHM) was extracted from the fit. The autocorrelation background is due to a small amount of SHG light leaking into the detector.

Fig. 3. Multiple soliton formation. Shown is a sequence of autocorrelation measurements for an intracavity power range from 0.8 to 3.8 mW. Autocorrelation traces have been normalized to one at zero delay.

to as SAM 1–3. These SAMs have been chosen to provide a deep modulation depth ΔR [9] together with a short response time τ_r ranging from 300 fs to 10 ps . Two different general designs have been used in pursuit of these competing goals. SAM 1–2 employ multiple quantum wells to achieve a high ΔR. In contrast to the entirely nonresonant SAM 2, the modulation depth of SAM 1 was further increased by embedding the quantum wells in a slightly resonant cavity. Finally, SAM 3 relies only on a resonant design to achieve a high ΔR and uses only a single quantum well. The saturation fluence F_{sat} [9], the modulation depth ΔR, nonsaturable losses ΔR_{ns}, and the dominant time constants of the pump probe response have been carefully measured and are compiled in Table I.

Operation with these SAMs leads to clean femtosecond mode-locked operation with pulse durations below 500 fs and time-bandwidth products in the range from 0.34 to 0.38. SAM 1 and 2 were operated slightly above the saturation fluence, i.e., the pulse fluence $F_p \approx 2F_{sat}$. We monitored the laser output power using a fast photodiode and an RF analyzer. A very low sideband content of the photocurrent spectra indicates that the laser is operating in CW mode-locked operation and is free of Q-switching artifacts. The optical spectra show only very faint indications of Kelly sidebands [10] owing to the short cavity length. An autocorrelation of the shortest observed pulse is shown in Fig. 2, with the corresponding optical spectrum shown in the inset. These pulses exhibit a 179-fs pulse duration and a 7.7-nm-wide spectrum. These results were obtained with SAM 1, i.e., the SAM with the deepest modulation depth. To the best of our knowledge, this is the shortest pulse duration ever achieved for a Nd-doped fiber laser that has been mode-locked by an SAM. The use of the much faster SAM 2, instead, only resulted in 220-fs-long pulses, which clearly underlines the importance of ΔR over all other SAM characteristics.

Mode-locking with SAM 1 and 2 resulted in output pulse energies of $E_{out} \approx 2.5$ pJ at a repetition rate of 117 MHz. Let us
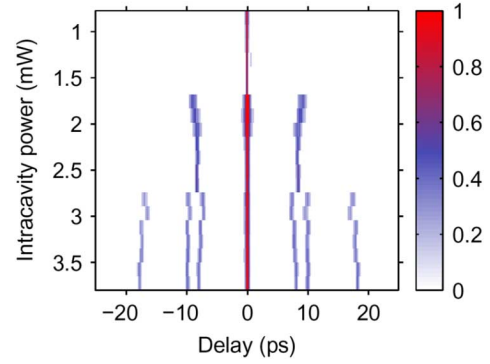
for simplicity neglect fiber gain and saturable absorption to see to what extent pulse formation in our laser is compatible with soliton solutions of the nonlinear Schrödinger equation. By considering output coupling and cavity losses, we estimate the average pulse energies in the MSF as $E_p = 3.5\,E_{out}$. Using this value and the full-width at half-maximum (FWHM) pulse duration τ, we can compute the soliton area $A = 0.56\,E_p\tau$ which yields $A = 0.8 \times 10^{-24}$ Js and 1.1×10^{-24} Js for SAM 1 and 2, respectively. Within a factor of about 3, these soliton areas are compatible with the theoretical estimate $A = |2\beta_2/\gamma| = 0.33 \times 10^{-24}$ Js, which may also be partially attributable to the limited experimental accuracy of the dispersion and nonlinearity measurements. However, this is in contrast to the behavior with SAM 3, where output pulse energies of up to 100 pJ were observed together with a pulse duration of $\tau = 400$ fs; i.e., these pulses show a soliton area that is about 200 times larger than for soliton operation [8].

Quite generally for SAM 1 and 2, we observe pulse energies slightly above the soliton energy. This slight but systematic deviation is understandable because the self-consistent pulse shape in our cavity is not only affected by the interplay of dispersion and self-phase modulation in the fiber, but it is modified by the strong saturable absorber action and by the fiber gain. Both effects will have an additional stabilizing action on the pulse. The saturable absorber action will delay pulse break up in the temporal domain and prevent the breakthrough of continuous wave emission [11]. The limited gain bandwidth will further restrict pulse broadening in the spectral domain, and therefore additionally stablizes the pulse. As long as the cavity supports self-consistent propagation of pulses, i.e., without changes in pulse shape upon subsequent round-trips, these pulses act like solitons, as is further outlined in Fig. 3. It should be pointed out that the additional pulse shaping effects may certainly explain deviations from an ideal fiber soliton up to a few 10% in terms of pulse duration and energy, but they cannot be held responsible for major deviations from the soliton scenario as were observed when using the strongly resonant SAM 3 and reported in [8]. The resonant structure of this SAM acts like a Gires–Tournois interferometer and introduces a dispersion of ≈ -4000 fs^2 into the cavity, which may hold an explanation for the greatly enhanced stable pulse energies observed when using SAM 3.

We further analyzed energy scaling of the soliton-like behavior with the slightly resonant SAM 1, as shown in Fig. 3. In this experiment, the pump power was slowly increased,
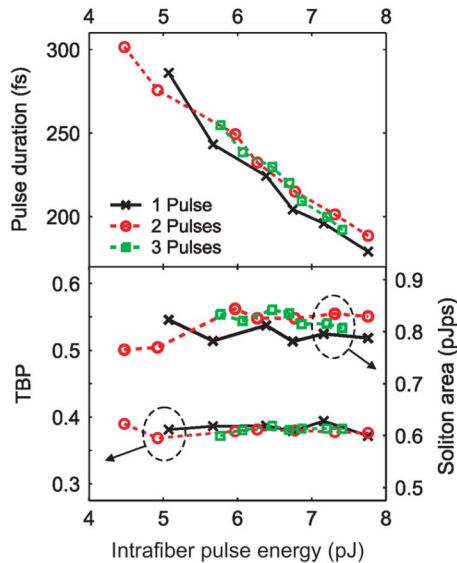
Fig. 4. Scaling of pulse duration τ, time-bandwidth product (TBP) and soliton area A with intrafiber pulse energy E_p. Black crosses and solid line: single pulse. Red circles and dashed line: double pulses. Green squares and dashed line: triple pulses.

recording autocorrelation and spectrum for each setting, with multisoliton formation eventually setting in. Stable pulse formation initiates at intracavity powers above 0.8 mW. Above 1.7 mW, two solitons at a distance of 9 ps form, and above 2.7 mW, three solitons copropagate (see Fig. 3). In the latter case, the three solitons do not share the same temporal distance, as indicated by the split autocorrelation sideband at 8–10 ps. Together with the peak at 18-ps delay, this autocorrelation is indicative of three pulses with delays of 8 and 10 ps between adjacent pulses. Repetition of the experiment does not exactly reproduce identical temporal distances. Nevertheless, the solitons always group at a preferred distance of about 10 ps, i.e., roughly 20 to 30 times their width, which practically excludes any direct interaction as there is negligible overlap between the individual pulses. Well-separated but stable bound solitons at some 10 to 20 pulsewidths were previously observed in fiber lasers with different topology [12], [13]. A long-range interaction mediated by dispersive waves [14] or soliton–soliton interactions in dissipative media [15] have been quoted as possible explanations for soliton forces on this length scale.

Fig. 4 shows the development of pulse duration τ with intracavity pulse energy. For the lowest observed pulse energies, we measured $\tau \approx 300$ fs. For the highest energies of 7.8 pJ, τ decreases to below 200 fs. Over the entire range of pulse energies and numbers, the time-bandwidth product stays unchanged at ≈ 0.38, indicating that pulse shape and chirp remain constant. Moreover, the soliton area $A \approx 0.8 \times 10^{-24}$ Js also remains unchanged over a wide parameter range at about twice the value anticipated for classical fiber solitons.

To the best of our knowledge, these experiments constitute the first demonstration of true solitons in a monolithic fiber laser medium that is operated in the neodymium gain band. This type of soliton is contrasted to the quasi-solitons prevailing in other types of solid-state lasers [16], [17] or compound fiber lasers incorporating normally dispersive fiber sections that do not support solitons by themselves [3], [6].

As we have shown, however, even the solitons in our laser show small but systematic deviations from freely propagating ones. These deviations are owing to self-amplitude modulation and also to the fiber gain. Still, these systematic deviations are typically within a factor 2 of soliton parameters. Apart from these fundamental aspects, the combination of rare-earth-doped MSFs with deep-modulation SAMs appears to be a viable alternative for simple femtosecond oscillators in the 1-μm range. Combining the mature SAM technology developed for solid-state lasers and soliton pulse shaping, such a source appears attractive as a compact femtosecond pulse source. Such a structurally very simple optical pulse source could find widespread application for amplifier chains operating in this wavelength range.

REFERENCES

[1] F. Adler, K. Moutzouris, A. Leitenstorfer, H. Schnatz, B. Lipphardt, G. Grosche, and F. Tauser, "Phase-locked two-branch Er-doped fiber laser system for long-term precision measurements of optical frequencies," *Opt. Express*, vol. 12, pp. 5872–5880, 2004.

[2] K. Tamura, E. P. Ippen, H. A. Haus, and L. E. Nelson, "77-fs pulse generation from a stretched-pulse mode-locked all-fiber ring laser," *Opt. Lett.*, vol. 18, pp. 1080–1082, 1993.

[3] F. Ö. Ilday, J. Chen, and F. X. Kärtner, "Generation of sub-100-fs pulses at up to 200 MHz repetition rate from a passively mode-locked Yb-doped fiber laser," *Opt. Express*, vol. 13, pp. 2716–2721, 2005.

[4] J. K. Ranka, R. S. Windeler, and A. J. Stentz, "Visible continuum generation in air silica microstructure optical fibers with anomalous dispersion at 800 nm," *Opt. Lett.*, vol. 25, pp. 25–7, 2000.

[5] P. St. J. Russell, "Photonic crystal fibers," *Science*, vol. 299, pp. 358–362, 2003.

[6] A. V. Avdokhin, S. V. Popov, and J. R. Taylor, "Totally fiber integrated, figure-of-eight, femtosecond source at 1065 nm," *Opt. Express*, vol. 11, pp. 265–269, 2003.

[7] A. Isomäki and O. G. Okhotnikov, "All-fiber ytterbium soliton mode-locked laser with dispersion control by solid-core photonic bandgap fiber," *Opt. Express*, vol. 14, pp. 4368–4373, 2006.

[8] M. Moenster, P. Glas, G. Steinmeyer, R. Iliew, N. Lebedev, R. Wedell, and M. Bretschneider, "Femtosecond Nd-doped microstructure fiber laser," *Opt. Express*, vol. 13, pp. 8671–8677, 2005.

[9] M. Haiml, R. Grange, and U. Keller, "Optical characterization of semiconductor saturable absorbers," *Appl. Phys. B*, vol. 79, pp. 331–339, 2004.

[10] S. M. J. Kelly, "Characteristic side-band instability of periodically amplified average soliton," *Electron. Lett.*, vol. 28, pp. 806–808, 1992.

[11] H. A. Haus, J. G. Fujimoto, and E. P. Ippen, "Structures for additive pulse mode-locking," *J. Opt. Soc. Amer. B*, vol. 8, pp. 2068–2076, 1991.

[12] N. H. Seong and D. Y. Kim, "Experimental observation of stable bound solitons in a figure-eight fiber laser," *Opt. Lett.*, vol. 27, pp. 1321–1323, 2002.

[13] D. Y. Tang, B. Zhao, and L. M. Zhao, "Soliton interaction in a fiber ring laser," *Phys. Rev. E*, vol. 72, no. 016616, 2005.

[14] K. Smith and L. F. Mollenauer, "Experimental observation of soliton interaction over long fiber paths: Discovery of a long-range interaction," *Opt. Lett.*, vol. 14, pp. 1284–1286, 1989.

[15] P. Grelu, F. Belhache, F. Gutty, and J. M. Soto-Crespo, "Relative phase locking of pulses in a passively mode-locked fiber laser," *J. Opt. Soc. Amer. B*, vol. 20, pp. 863–870, 2003.

[16] T. Brabec, C. Spielmann, and F. Krausz, "Mode locking in solitary lasers," *Opt. Lett.*, vol. 16, pp. 1961–1963, 1991.

[17] F. X. Kärtner, I. D. Jung, and U. Keller, "Soliton mode-locking with saturable absorbers," *IEEE J. Sel. Top. Quantum Electron.*, vol. 2, no. 3, pp. 540–556, Sep. 1996.